Use of analytical techniques for the identification of the morphology of geopolymers

Dimitra Zaharaki [1*], Kostas Komnitsas[1] and Georgios Bartzas[2]

[1]School of Mineral Resources Engineering, Technical University of Crete, Chania, 73100, Greece

[2]School of Mining and Metallurgical Engineering, National Technical University of Athens, Zografos Campus, Athens, 15780, Greece

*Corresponding author email: zaharaki@mred.tuc.gr, tel: +30 2821037864, fax: +30 2821069554

Abstract

The present study highlights the importance of the use of analytical techniques for the identification of the morphology and structure of geopolymers. As an example, geopolymers produced from ferronickel slag and the three main components of construction and demolition wastes (CDW), namely bricks, tiles and concrete, were used. Geopolymers were synthesized by alkali activation of the starting materials using NaOH and Na_2SiO_3 solutions. Slag, bricks and tiles were successfully geopolymerized reaching a compressive strength higher than 50 MPa, while limited geopolymerization potential was obtained for concrete-based geopolymers (strength 13 MPa). The use of analytical techniques, X-ray Diffraction (XRD), Scanning Electron Microscopy (SEM), Fourier Transform Infrared Spectroscopy (FTIR) and Thermogravimetric analysis (TG) provided significant insights on the geopolymerization mechanisms, the mineralogy, the microstructure and indicate optimum synthesis conditions for each raw material used.

Keywords

Geopolymer, morphology, strength, XRD, SEM, FTIR, TG

Introduction

Geopolymers are partially or fully amorphous polymeric structures consisting of a network of SiO_4 and AlO_4 tetrahedra. Their synthesis involves reactions between aluminosilicates and concentrated caustic alkali metal silicate solution at ambient temperature. During the last two decades, various wastes such as fly ash, slag and red mud have been extensively investigated as potential raw materials for geopolymerization. The properties of geopolymers such as high early strength, thermal stability and corrosion resistance, depend strongly on the properties of the raw materials (Davidovits 1998, Komnitsas & Zaharaki 2007).

The complex reactions during alkaline activation of the starting materials may be explained by the values of the molar Si/Al and other ion ratios. Also a number of simple or advanced techniques may be used to obtain maximum information and elucidate geopolymerisation mechanisms. X-ray Diffraction (XRD) may be a useful tool despite the substantial amorphous nature of geopolymers, providing data regarding the extent to which crystalline starting materials have reacted. Scanning electron microscopy (SEM) allows a good description of the microstructure of geopolymers that could not be detected by other techniques. Fourier Transform Infrared Spectroscopy (FTIR) provides information about the vibrational transitions and rigidity of geopolymeric bonds. Thermogravimetric analysis (TG) can be used to assess the rates of water evaporation or identify the mechanism by which the specimens lose weight as a result of controlled heating (Duxson et al. 2006, Hanjitsuwan et al. 2014).

In the present study, XRD, SEM, FTIR and TG were used to provide significant insights on the geopolymerization mechanisms, the mineralogy, the microstructure and the properties of the geopolymers produced from ferronickel slag and the three main components of construction and demolition wastes (CDW), namely concrete, bricks and tiles.

Materials and methodology

The materials used in the present study are: electric arc slag produced at the LARCO S.A. ferronickel plant in Greece and CDW (concrete, bricks and tiles) collected from various demolished buildings. Raw materials were dried and pulverized using a BICO pulverizer Type UA and a FRITSCH pulverizer (Germany) and homogenized prior to use. Grain-size analysis of raw materials was performed using a Mastersizer S (Malvern Instruments) particle size analyzer (slag: <120 μm and d_{50} 12 μm, bricks: <140 μm and d_{50} 7 μm, tiles: <140 μm and d_{50} 14 μm, concrete: <190 μm and d_{50} 10 μm). Table 1 shows the chemical composition of the raw materials used in the form of oxides, as derived from the use of an X-ray fluorescence energy dispersive spectrometer Bruker-AXS S2 Range type.

Table 1. Chemical composition (%) of the raw materials

	Slag (S)	Bricks (B)	Tiles (T)	Concrete (C)
Na_2O	-	1.03	-	0.57
MgO	2.76	4.75	4.46	4.21
K_2O	-	2.80	1.37	1.26
CaO	3.73	8.79	8.78	65.42
Fe_2O_3	43.83	6.00	5.39	0.75
Al_2O_3	8.32	14.95	9.80	1.49
SiO_2	32.74	57.79	70.54	5.81
MnO	0.41	0.05	0.06	0.01
SO_3	0.45	-	-	0.82
TiO_2	-	0.85	0.77	0.03
LOI*	-	1.89	0.23	21.59
Sum	95.31**	98.89	101.41	101.95

*loss on ignition by heating at 1050 °C for 4h
**Cr_2O_3: 3.07%

Geopolymers were synthesized by mixing the raw materials under continuous stirring with the alkaline solution prepared by dissolving NaOH anhydrous pellets (ACS-ISO for analysis) in distilled water and sodium silicate solution (Merck, Na_2O=7.5-8.5%, SiO_2=25.5-28.5%). The experimental methodology is described in detail in Komnitsas et al. (2014). The specimens produced were subjected to compressive strength testing using a MATEST C123N load frame.

XRD analysis of the raw materials and geopolymers was performed using a Bruker D8 Advance diffractometer (Cu tube, scanning range from 3° to 70° 2θ, step 0.03°, measuring time 4s/step) and the qualitative analysis using the DIFFRACplus Software (Bruker AXS). SEM analysis was carried out with a JEOL 6380LV scanning electron microscope equipped with an EDS INCA microanalysis system with low vacuum, pressure 30 Pa, voltage 20 kV and 10-12 mm working distance from the detector. FTIR analysis on pellets produced after mixing of each sample with KBr at a ratio 1:100 w/w, was carried out with a Perkin-Elmer Spectrum 1000 (USA). TG analysis was done using a differential thermogravimetric analyzer Diamond DTA-TG of Perkin Elmer (temperature range 40-850 ºC, measurement precision ±2ºC, microbalance sensitivity <5 μg, atmospheric pressure, nitrogen atmosphere, flow rate 100 mL/min, heating rate 10 ^{o}C/min).

Results and discussion

Geopolymerization potential of the raw materials

Slag, bricks and tiles can be successfully geopolymerized reaching a compressive strength of 50-58 MPa, while lower strength (13 MPa) was obtained for concrete-based geopolymers, as discussed in detail in previous studies (Komnitsas et al. 2013, 2014). The optimum synthesis conditions as well as selected molar ratios of oxides in the initial paste are shown in Table 2. High SiO_2/Al_2O_3 ratios, as in tiles (12.67), result in high compressive strength. Bricks and slag that have lower SiO_2/Al_2O_3 ratio acquire lower strengths. Also high $SiO_2/(Al_2O_3+CaO)$ ratios (4.81, 4.03 and 3.30 for tile, slag and brick geopolymers, respectively) result in higher compressive strength. If the content of CaO is high, as in concrete, the $SiO_2/(Al_2O_3+CaO)$ ratio is quite low (0.12) and despite the high SiO_2/Al_2O_3 ratio (9.86) geopolymers with low compressive strength are produced. Optimum values of the $H_2O/(Na_2O+K_2O)$ ratios, correspond to the presence of sufficient water to participate in geopolymeric reactions and thus high compressive strength is acquired.

Table 2. Optimum conditions for the synthesis of slag (S), brick (B), tile (T) and concrete (C) based geopolymers and molar ratios of oxides of the initial paste

	S	**B**	**T**	**C**
Max strength, MPa	52	50	58	13
NaOH, M	8	8	10	14
Temperature, °C	80	90	80	90
SiO_2/Al_2O_3	7.33	6.84	12.67	9.86
$SiO_2/(Al_2O_3+CaO)$	4.03	3.30	4.81	0.12
$H_2O/(Na_2O+K_2O)$	8.30	8.32	9.03	6.62
$(Na_2O+K_2O)/SiO_2$	0.10	0.14	0.12	1.53
$SiO_2/(Al_2O_3+Fe_2O_3)$	1.68	5.44	9.38	7.47

These ratios as well as the results from XRD, FTIR, SEM and TG analyses, as discussed in the following section, provide very useful insights on the geopolymerization mechanisms and the microstructure of the final products.

XRD, SEM, FTIR and TG analyses

Figure 1 shows the XRD patterns of geopolymers synthesized from slag (S), bricks (B), concrete (C) and tiles (T) under the optimum synthesis conditions. Partially reacted or unreacted crystalline phases, such as quartz, calcite, fayalite and albite present in geopolymers are also detected in the raw materials. This partial dissolution is also indicated by the decrease of the intensity of the crystalline peaks compared to the respective peaks of the raw materials. The only new phase detected in CDW geopolymers is pirssonite ($Na_2Ca(CO_3)_2.2H_2O$), which is an evaporite formed as a result of atmospheric carbonation. Its formation in concrete-based geopolymers as a result of the high CaO content in concrete (close to 65%) and the consumption of Na ions from the activating solution, inhibits the development of geopolymeric bonds.

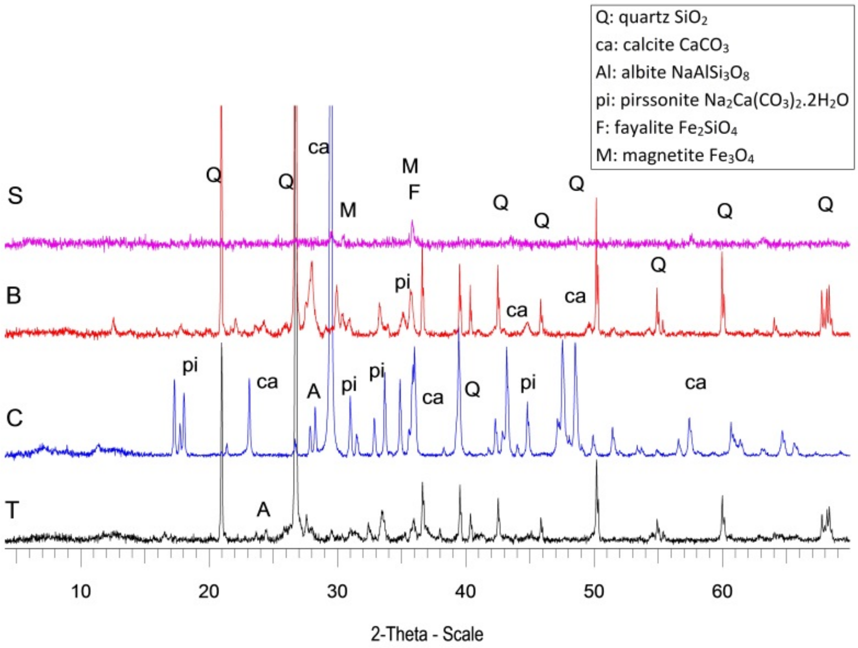

Figure 1. XRD patterns of geopolymers synthesized from slag (S), bricks (B), concrete (C) and tiles (T)

In Figure 2, SEM images of geopolymers synthesized from slag, bricks, tiles and concrete are illustrated. The image of slag-based geopolymer shows a matrix consisting of slag grains and the geopolymeric gel that acts as a binder and enhances the compressive strength of the specimens. In brick-based geopolymer, the geopolymeric structure is characterized by a certain degree of homogeneity that improves the final strength. The high content of Si and Al as derived from EDS analysis (not shown) confirms these findings. In tile-based geopolymer a geopolymeric structure is also present as also confirmed by the high content of dissolved Si and Al. The matrix of concrete-based geopolymer is heterogeneous and grains of various sizes are detected, indicating partial reaction of initial concrete during alkali-activation and thus lower compressive strength. As also deduced from EDS analysis, Ca is the main component detected (white areas shown in Figure 2, lower row, left), while Si and Al, which are the main elements required for the formation of geopolymeric bonds, are found in smaller quantities.

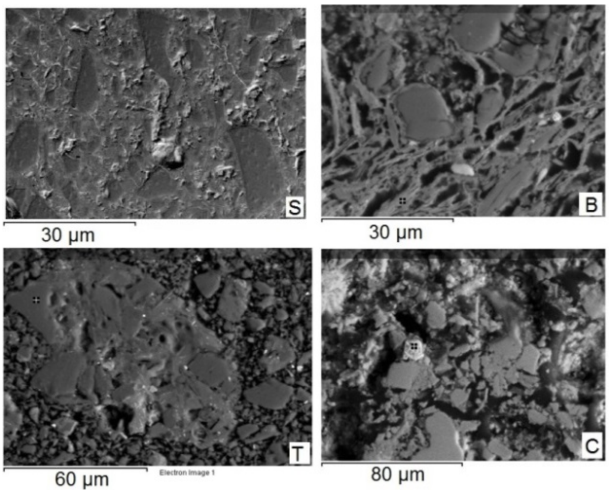

Figure 2. SEM images of geopolymers synthesized from slag (S), bricks (B), tiles (T) and concrete (C)

Figure 3 shows the FTIR spectra of the initial components (slag, concrete, bricks and tiles) as well of the produced geopolymers. Stretching and bending H–O–H vibrations are assigned to the small bands between 1800 and 3350 cm^{-1} as well as at 1630 cm^{-1}, due to the weak bonds of H_2O molecules adsorbed on the surface of the specimens. A doublet of peaks seen at around 1490 and 1420 cm^{-1} for all geopolymers is due to atmospheric carbonation, asymmetric stretching and out of plane bending modes of CO_3. It is noticed that these bands are quite strong mainly in concrete and also in concrete-based geopolymer that acquires the lowest strength (13 MPa) and are attributed to the modes of CO_3 contained in $CaCO_3$, as also confirmed by XRD analysis. The strong peak at 876 cm^{-1} also is due to out of plane bending of CO_3.

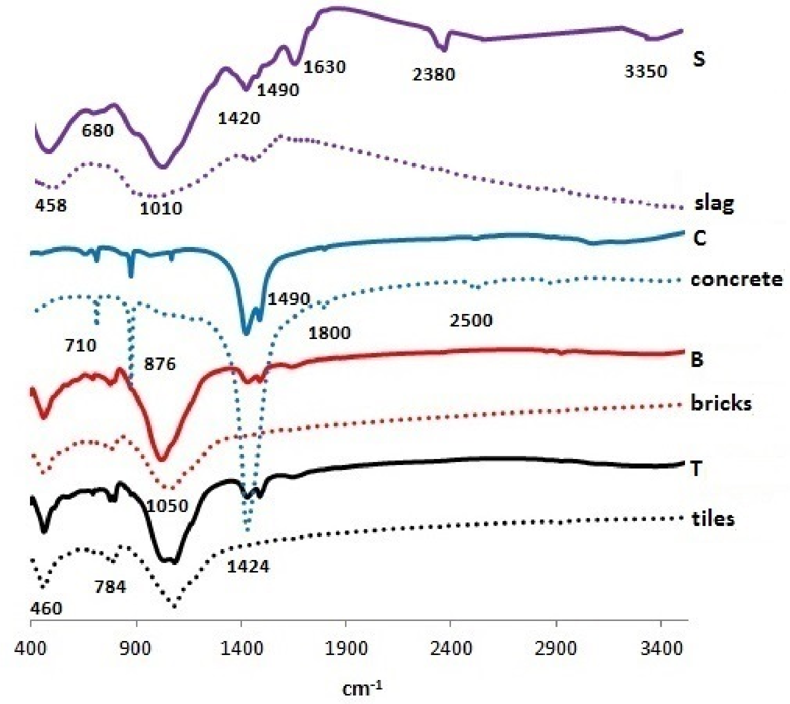

Figure 3. FTIR spectra of the initial components and the geopolymers synthesized from slag (S), bricks (B), concrete (C) and tiles (T)

The broad peaks at around 1000 cm^{-1} shown in geopolymers produced from slag, bricks and tiles are major fingerprints of the geopolymeric matrix and are attributed to Si–O stretching, Si–O–Si and Al–O–Si asymmetric stretching vibrations during geopolymerisation. These peaks indicate the formation of an amorphous aluminosilicate gel due to dissolution of raw materials under highly alkaline conditions. The same peaks, slightly shifted, are also present in slag, bricks and tiles in lower intensity though. No such peaks are shown either in concrete or concrete-based geopolymer that acquire the lowest strength. The other peaks at around 450-780 cm^{-1} are assigned to bending Si–O–Si and O–Si–O vibrations (Socrates 2001).

Figure 4 shows the TG curves representing the % weight decrease versus temperature, for the geopolymers produced from slag, concrete, bricks and tiles. For slag-, brick- and tile-based geopolymers water is gradually lost. Up to 200 ◦C the absorbed water loss is 4, 8 and 9%, while the remaining water seems to be bound tightly in the geopolymeric channels and evaporates slowly, thus the total water loss is just 8, 9 and 12 %, respectively.

A different behaviour is shown for concrete-based geopolymers; 9% of the absorbed water is lost at around 200 ◦C, a sharper water loss of 36% is recorded at around 600 ◦C due to decomposition of calcite and thereafter water loss is continuous and reaches 42%. It is mentioned that an optimum water content should be present in the initial paste, so that the geopolymeric structure $M_n((SiO_2)_z–AlO_2)_n.wH_2O$ is formed and geopolymers acquire a noticeable strength.

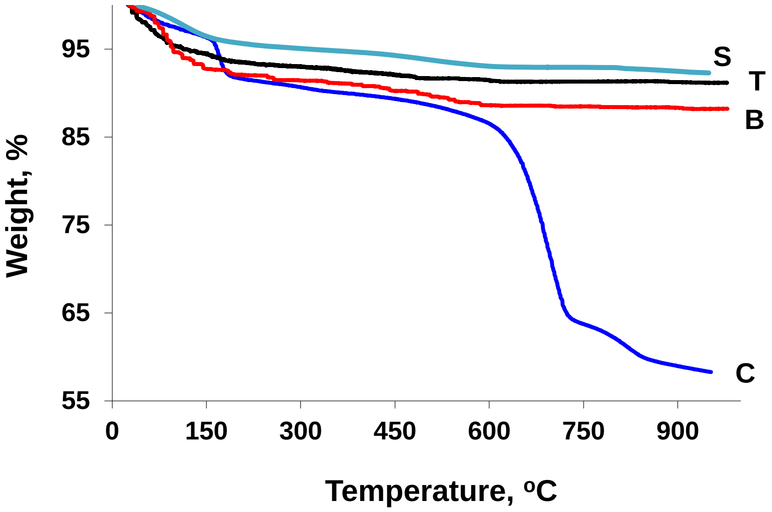

Figure 4. TG curves of geopolymers synthesized from slag (S), bricks (B), concrete (C) and tiles (T)

Conclusions

The use of analytical techniques, XRD, SEM, FTIR and TG, contributes significantly to the complete characterisation of the microstructure of geopolymers. Slag, bricks and tiles which were successfully geopolymerized and acquired strength higher than 50 MPa, are characterized by a homogenous structure. This structure consists of an amorphous aluminosilicate gel which is formed due to adequate water content and dissolution of Si and Al from the raw materials under highly alkaline conditions. Concrete is rather poorly geopolymerized and specimens are characterized by an inhomogeneous matrix where unreacted grains are present. The limited content of Si and Al in the gel is due to the incomplete dissolution of the aluminosilicate matrix while the identification of pirssonite indicates the consumption of the alkaline activator.

Acknowledgements

The present study has been co-funded by the European Commission (European Regional Development Fund) and by national funds through the Operational Programme “Competitiveness and Entrepreneurship” (OPCE II 2007 - 2013), National Strategic Reference Framework – Research funded project: “Recycling of quarry dust and construction and demolition wastes for the production of novel ecological building elements”, DURECOBEL 11SYN_8_584, in the framework of the Action COOPERATION 2011– Partnerships of Production and Research Institutions in Focused Research and Technology Sectors.

References

Davidovits, J. (1998) Geopolymer chemistry and properties. In: Davidovits J, and Orlinski J. (eds.). Proceedings of the 1st International Conference Geopolymer '88, Compiegne, France, 1-3 June, pp. 25-48.

Duxson, P., Lukey, G.C., & Van Deventer, J.S.J. (2006) Nanostructural design of multifunctional geopolymeric materials. Ceramic Transactions, 175, 203-214

Hanjitsuwan, S., Hunpratub, S., Thongbai, P., Maensiri, S., Sata, V., & Chindaprasirt, P. (2014) Effects of NaOH concentrations on physical and electrical properties of high calcium fly ash geopolymer paste. Cement & Concrete Composites, 45, 9-14

Komnitsas, K., & Zaharaki, D. (2007) Geopolymerisation: A review and prospects for the minerals industry. Minerals Engineering, 20, 1261-1277

Komnitsas, K., Zaharaki, D., & Bartzas, G. (2013) Effect of sulphate and nitrate anions on heavy metal immobilisation in ferronickel slag geopolymers. Applied Clay Science, 73, 103-109

Komnitsas, K., Zaharaki, D., Vlachou, A., Bartzas, G., & Galetakis, M. (2014) Effect of synthesis parameters on the quality of construction and demolition wastes (CDW) geopolymers. Advanced Powder Technology, 26, 368-376

Socrates, G. (2001) Infrared and Raman Characteristic Group Frequencies. 3rd edition, John Wiley & Sons Ltd, England.